Electron-impact ionization of all ionization stages of beryllium

J. Colgan, S. D. Loch, and M. S. Pindzola

Department of Physics, Auburn University, Auburn, Alabama 36849, USA

C. P. Ballance and D. C. Griffin

Department of Physics, Rollins College, Winter Park, Florida 32789, USA

Efforts to provide accurate atomic collisional data for use in fusion plasma models have been extended to provide electron-impact ionization cross sections for all stages of beryllium. Ionization cross sections are presented from the ground and first excited states of Be, Be^+, Be^{2+}, and Be^{3+}. For all cases, two perturbative distorted-wave methods are used to calculate the ionization cross section. For Be, Be^+, and Be^{2+}, the nonperturbative time-dependent close-coupling and the R matrix with pseudostates methods are used to calculate the ionization cross sections. R matrix with pseudostates calculations are also presented for Be^{3+}. In general, the two nonperturbative methods are in good agreement with each other for electron-impact ionization of Be, Be^+, and Be^{2+}. Furthermore, for ionization from the ground and the first excited states of Be and the first excited state of Be^+, the perturbative distorted-wave calculations are significantly higher than the nonperturbative calculations. The atomic level resolved rate coefficients generated in this work have been archived and will be used to increase the accuracy of collisional-radiative modeling for beryllium.

PACS number(s): 34.80.Kw

I. INTRODUCTION

The increasing use of light elements, such as helium, lithium, and beryllium as constituents of plasma facing components and as diagnostic tools in fusion plasma devices challenges plasma modelers to provide accurate simulations of the complex physical processes inherent in fusion plasmas. Lithium has been used extensively as a plasma diagnostic [1] and helium is used both for heating and diagnostics in several fusion plasma devices. Recent theoretical studies of the electron-impact excitation and ionization of lithium and its ions [2] highlighted the need for a comprehensive review of the lithium database, and this has now been completed [3].

Recently, beryllium has been proposed as a first wall component for the plasma-facing material in the planned ITER experiment [4], due to its low Z and strong radiation properties at the low electron temperatures present in the divertor. These applications have focused interest on the atomic data used to model the interactions with fusion plasmas. However, there exists little experimental or theoretical data for the electron-impact excitation or ionization of beryllium and its ions. There have been few experimental efforts to obtain cross sections for excitation or ionization of beryllium or its ions, due to its toxic nature. Only one set of experimental measurements for the electron-impact ionization of Be^+ [6] seems to exist in the literature.

On the theoretical side, studies of the elastic electron-beryllium scattering cross sections have been made by Fursa and Bray [7,8] using the convergent close-coupling (CCC) method. They also provided electron-impact ionization cross sections from the ground state. These followed earlier calculations using the R matrix with pseudostates (RMPS) method by Bartschat *et al.* [9,10] of inelastic excitations into the low-lying states of neutral beryllium. Overall, these two methods were found to be in good agreement and the effect of coupling to the target continuum was found to be important,

especially for optically forbidden transitions.

A previous set of calculations for the electron-impact ionization of the ground state of Be^+ has also been made by Pindzola *et al.* [11]. Here, time-dependent close-coupling (TDCC) calculations were compared to time-independent R matrix with pseudostates calculations; very good agreement was found between the two sets of nonperturbative calculations, which were both lower than the only existing experimental measurements of Falk and Dunn [6] by more than 30%. A study of comparisons between RMPS and CCC calculations by Bartschat and Bray [12] came to similar conclusions: the nonperturbative theories, while in very good agreement with each other, were consistently lower than the only available experimental measurements.

In this paper, we present ionization cross sections from the ground and first excited configurations of neutral Be, Be^+, Be^{2+}, and Be^{3+}. Ionization cross sections from excited configurations calculated by nonperturbative methods have been shown to differ greatly from perturbative calculations [13,14] for neutral species. Also, the large cross sections for ionization from excited configurations can significantly affect ionization rate coefficients and population models.

Perturbative distorted-wave calculations are presented for all systems and the nonperturbative TDCC method is used to calculate the ionization cross sections for all ions except Be^{3+}, where for this three times ionized system, perturbative calculations are expected to be fairly accurate. RMPS calculations are made for all ions. The distorted-wave calculations were made using a configuration-average set of programs [15] which have been used in calculations of ionization cross sections for many atomic systems.

The TDCC theory was first introduced for electron scattering in the calculation of the electron-impact ionization of hydrogen [16,17]. It has since been applied to a wide variety of electron-impact excitation and ionization calculations (see

Ref. [18] for a recent review). The *R*-matrix programs used to perform the RMPS calculations are modified versions of the RMATRXI [19] codes. They have been implemented for distributed-memory parallel computers, and include the orthogonalization procedure between pseudostate and continuum orbitals as developed by Gorczyca and Badnell [20]. These codes have already been used extensively in studies of electron-impact ionization [13,21] and excitation [22,23] of other atomic ions.

In the following section, we give a short overview of the distorted-wave, TDCC, and RMPS theories as applied to the electron-impact ionization of Be and its ions. We then present cross sections for electron-impact ionization of all Be ions and compare our nonperturbative results with distorted-wave calculations, as well as other calculations, where available. In Sec. IV, we discuss efforts that will be required to address the atomic data needs of fusion plasma modelers.

II. THEORETICAL METHODS

A. The time-independent distorted-wave method

The configuration-average distorted-wave expression for the direct ionization cross section of the $(n_t l_t)^{w_t}$ subshell of any atom is given [15] by

$$\sigma = \frac{32 w_t}{k_i^3} \int_0^{E/2} \frac{d\left(\frac{k_e^2}{2}\right)}{k_e k_f} \sum_{l_i, l_e, l_f} (2l_i+1)(2l_e+1)$$
$$\times (2l_f+1) \mathcal{P}(l_i, l_e, l_f, k_i, k_e, k_f), \qquad (1)$$

where the linear momenta (k_i, k_e, k_f) and the angular momentum quantum numbers (l_i, l_e, l_f) correspond to the incoming, ejected, and outgoing electron, respectively. The total energy $E = (k_i^2/2) - I = (k_e^2/2) + (k_f^2/2)$, where I is the subshell ionization energy. The first-order scattering probability is given [15] by

$$\mathcal{P}(l_i, l_e, l_f, k_i, k_e, k_f)$$
$$= \sum_\lambda A^\lambda_{l_i, l_e, l_f} [R^\lambda(k_e l_e, k_f l_f, n_t l_t, k_i l_i)]^2$$
$$+ \sum_{\lambda'} B^{\lambda'}_{l_i, l_e, l_f} [R^{\lambda'}(k_f l_f, k_e l_e, n_t l_t, k_i l_i)]^2$$
$$+ \sum_\lambda \sum_{\lambda'} C^{\lambda, \lambda'}_{l_i, l_e, l_f} R^\lambda(k_e l_e, k_f l_f, n_t l_t, k_i l_i) R^{\lambda'}$$
$$\times (k_f l_f, k_e l_e, n_t l_t, k_i l_i), \qquad (2)$$

where the angular coefficients A, B, C may be expressed in terms of standard $3-j$ and $6-j$ symbols, and R^λ are standard radial Slater integrals.

The radial distorted waves $P_{kl}(r)$ needed to evaluate the Slater integrals are solutions to a radial Schrödinger equation given by

$$\left(h(r) - \frac{k^2}{2} \right) P_{kl}(r) = 0, \qquad (3)$$

where

$$h(r) = -\frac{1}{2} \frac{d^2}{dr^2} + \frac{l(l+1)}{2r^2} - \frac{Z}{r} + V_D(r) + V_X(r), \qquad (4)$$

and Z is the atomic number. The direct V_D potential is given by

$$V_D(r) = \sum_u^{occ} w_u \int_0^\infty \frac{P^2_{n_u l_u}(r')}{\max(r', r)} dr', \qquad (5)$$

where the $P_{n_u l_u}(r)$ are configuration-average Hartree-Fock bound radial orbitals [24]. The exchange V_X potential is calculated in a local-density approximation [25]. The incident- and scattered-electron continuum orbitals are evaluated in a V^N potential, while the ejected continuum orbital is calculated in a V^{N-1} potential [5], where $N = \Sigma_u w_u$ is the total number of target electrons. These calculations are listed as DWIS(N) (distorted-wave with incident and scattered electrons calculated in V^N potentials) in the following sections. The DWIS(N) method has proved especially accurate for high angular momentum scattering. A second set of calculations was also made where the incident, scattered, and ejected electrons were calculated in a V^{N-1} potential [26], listed as DWIS($N-1$) in subsequent sections. This method is generally more accurate for low-angular-momentum scattering. The continuum normalization for all distorted waves is one times a sine function.

B. The time-dependent close-coupling method

The configuration-average time-dependent close-coupling expression for the direct ionization of the $(n_t l_t)^{w_t}$ subshell of any atom is given [17,27] by

$$\sigma = \frac{w_t \pi}{4(2l_t+1)k_i^2} \int_0^E \frac{d\left(\frac{k_e^2}{2}\right)}{k_e k_f} \sum_{l_i, l_e, l_f} \sum_{L, S} (2L+1)(2S+1)$$
$$\times \mathcal{P}(l_i, l_e, l_f, L, S, k_i, k_e, k_f), \qquad (6)$$

where L is the angular-momentum quantum number obtained by coupling l_t and l_i (or l_e and l_f) and S is the spin momentum quantum number obtained by coupling two spin-$\frac{1}{2}$ electrons. The scattering probability is obtained by projecting the two-dimensional radial wave function $P^{LS}_{l_1 l_2}(r_1, r_2, t)$ onto appropriate products of bound and continuum radial orbitals at a suitable time after the collision.

The radial wave functions $P^{LS}_{l_1 l_2}(r_1, r_2, t)$ are solutions to the time-dependent radial Schrödinger equation given by

$$i\frac{\partial P_{l_1 l_2}^{LS}(r_1, r_2, t)}{\partial t} = T_{l_1 l_2}(r_1, r_2) P_{l_1 l_2}^{LS}(r_1, r_2, t)$$

$$+ \sum_{l_1', l_2'} U_{l_1 l_2, l_1' l_2'}^{L}(r_1, r_2) P_{l_1' l_2'}^{LS}(r_1, r_2, t),$$

$$(7)$$

where expressions for the quantities $T_{l_1 l_2}(r_1, r_2)$ and $U_{l_1 l_2, l_1' l_2'}^{L}(r_1, r_2)$ can be found in Ref. [27]. The radial wave function at a time $t = T$ following the collision is obtained by propagating the time-dependent close-coupling equations on a two-dimensional finite lattice. The two-electron wave functions fully describe the correlation between the ejected and scattered electrons at all times following the collision.

The bound and continuum radial orbitals required to describe the initial state and for projection can be obtained by diagonalization of the Hamiltonian $h(r)$ of Eq. (4) on a one-dimensional finite lattice. The direct (V_D) and local exchange (V_X) potentials are constructed as pseudopotentials in which the inner nodes of the valence Hartree-Fock orbitals are removed in a smooth manner. This prevents unphysical excitation of filled subshells during time propagation of the close-coupled equations [28]. The Fourier-transform method [29], used to extract the ionization cross section for many incident electron energies for only one time propagation of the Schrödinger equation, is employed to obtain cross sections over a wide range of energies around the peak of the ionization cross sections.

C. The *R*-matrix with pseudostates method

The RMPS method excels in providing many energy points from the ionization threshold onward and in giving the ionization cross sections from the ground and metastable terms in a single calculation; it has been described in detail elsewhere (e.g., Refs. [21,30]). In our implementation of this method, the target continuum is represented by a set of non-orthogonal Laguerre pseudo-orbitals that are generated using the program AUTOSTRUCTURE [31]. These orbitals are then orthogonalized with respect to the spectroscopic orbitals and with each other. With the exception of neutral beryllium, spectroscopic orbitals were employed only for those states from which we determined ionization cross sections. However, the RMPS calculation for the neutral atom is very large and we plan to use the same calculation to study electron-impact excitation of beryllium. For this reason, spectroscopic orbitals were employed through $n = 4$.

Extensive pseudostate bases were used in an effort to converge the ionization cross sections from the ionization threshold to at least four times this energy for the neutral and singly ionized species, and twice this energy for the doubly and triply ionized species. In the case of the ions, a variety of calculations involving different expansions of spectroscopic and pseudostate terms were performed and compared in order to ensure consistency between different models. The ionization cross sections were determined from the sum of the cross sections to those pseudostates above the ionization threshold.
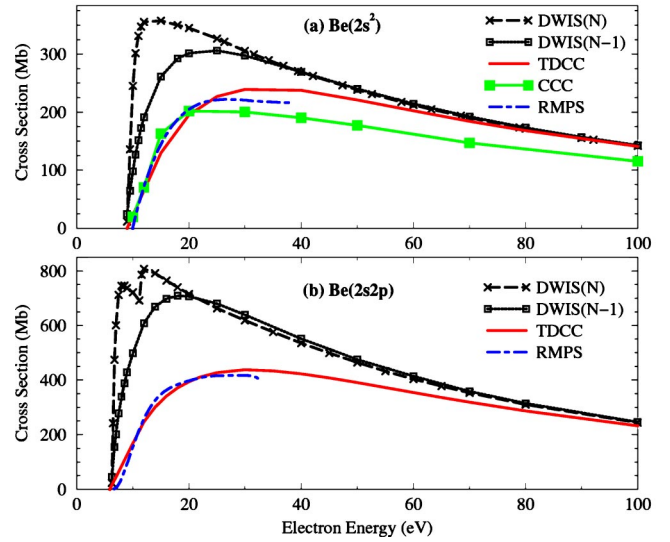

FIG. 1. Electron-impact ionization cross sections for neutral Be, from (a) the ground $1s^2 2s^2$ configuration and (b) the first excited $1s^2 2s 2p$ configuration. The solid lines are the time-dependent close-coupling calculations. The dot-dashed lines are the RMPS calculations and the short-dashed (with crosses) and dotted lines (with squares) are the DWIS(N) and DWIS$(N-1)$ calculations, respectively. The solid line with squares are CCC calculations from Ref. [7]. In (b) all calculations include ionization from both the $2s$ and $2p$ subshells. Also, the RMPS calculations are for ionization from the $1s^2 2s 2p$ ^3P term only (1.0 Mb $= 1.0 \times 10^{-18}$ cm^2).

The final models used for all RMPS calculations of the ions of beryllium employed pseudo-orbitals ranging in principal quantum number up to 14 and orbital angular momentum from 0 to 4. Including more pseudo-orbitals, rather than their spectroscopic equivalent, proved beneficial in two ways: First, the ionization cross sections had less "ripples" from pseudoresonances due to more complete pseudostate bases. Second, the size of the *R*-matrix box for ions is largely determined by the radial extent of the spectroscopic orbitals; thus by using pseudo-orbitals for all principal quantum numbers above $n = 2$, the $(N+1)$-electron continuum basis could be kept relatively small, allowing us to calculate cross sections to higher energies. Because of the size of the RMPS calculation for neutral beryllium, a more limited representation of the target continuum was necessary. Pseudostates were used from $n = 5$ to $n = 11$ for the $2snl$ configurations and from $n = 5$ to $n = 10$ for the $2pnl$ configurations, again with l ranging from $l = 0$ to $l = 4$.

III. RESULTS

A. Electron-impact ionization of Be($1s^2 2s^2$) and ($1s^2 2s 2p$)

In Fig. 1, we show the electron-impact ionization cross sections for neutral beryllium, from (a) the ground $1s^2 2s^2$ configuration and (b) the first excited $1s^2 2s 2p$ configuration. Our TDCC calculations were made using a uniform mesh with mesh spacing of $\Delta r = 0.2$ with 512 mesh points. Partial-wave ionization cross sections were calculated for $L = 0-6$ and then "topped up" with distorted-wave [DWIS(N)] calculations for higher L up to $L = 50$. The DWIS(N)

method was used for the top-up as it is known to be more accurate for higher-angular-momentum states. We also carried out further TDCC calculations up to $L=10$ for selected electron energies as a check on the accuracy of our top-up; these extended calculations differed by at most 5% at the highest electron energies shown in Fig. 1. The Fourier-transform method [29] was employed to extract ionization cross sections at a wide range of energies around the peak of the cross section, from incident electron energies of 15 to 100 eV. A pseudopotential was employed to construct the $2s$ orbital for scattering from the ground state of beryllium to avoid unphysical filling of the $1s$ orbital. By a suitable adjustment of the coefficient of the local exchange potential V_X, the ionization threshold from the ground state of beryllium is tuned to the experimental value of 9.32 eV [32]. For electron scattering from the first excited configuration of beryllium ($1s^2 2s 2p$), the $2p$ orbital was calculated in a Hartree-Slater potential constructed using the $2s$ pseudo-orbital. This gave a configuration-average ionization threshold of 5.95 eV, again in good agreement with the experimental value [32]. We comment that, for ionization from the $2p$ subshell of the excited $2s 2p$ configuration, three times as many angular-momenta channels are required due to the $l_t = 1$ nature of the target. We also performed TDCC calculations for ionization from the $2s$ subshell of the $2s 2p$ configuration, leaving the ion in the $1s^2 2p$ configuration. In this case, the configuration-average ionization threshold was found to be 9.92 eV, in good agreement with the configuration-average experimental value.

As mentioned in the preceding section, the RMPS calculation was performed using spectroscopic orbitals for all $2snl$ and $2pnl$ configurations up to $n=4$ and pseudo-orbitals for all $2snl$ configurations from $n=5$ to $n=11$ and all $2pnl$ configurations from $n=5$ to $n=10$, for a total of 280 terms. We employed 45 basis orbitals to represent the $(N+1)$-electron continuum, and the size of the R-matrix box was 71.7 a.u.

In Fig. 1(a), our nonperturbative calculations are compared with two sets of distorted-wave calculations, DWIS(N) and DWIS($N-1$), as previously discussed. The TDCC calculations and the distorted-wave calculations have peaks at different electron energies, and the TDCC calculations are considerably lower in magnitude in this region. However, by 80 eV and above (over five times the ionization threshold), both sets of distorted-wave calculations are in good agreement with the TDCC calculations, since for the higher energies considered, the cross section will be dominated by contributions from the higher partial waves.

In Fig. 1 we also show RMPS calculations for ionization from (a) the ground state and (b) in the metastable $2s 2p$ ^3P term of beryllium. For ionization from the ground state, the TDCC and RMPS calculations are in fairly good agreement, with the RMPS results about 9% below those from the TDCC calculation near the peak in the ionization cross section. In Fig. 1(a) we also compare with CCC calculations from Ref. [7]. These, while showing good agreement in the low-energy region (around 20 eV) with the TDCC and RMPS calculations, are lower than the TDCC calculations by about 20% at higher energies. It also appears that the CCC

and RMPS calculations peak at a slightly lower energy than the TDCC calculation. Interestingly, the RMPS calculations seem to bisect the difference between the TDCC and CCC calculations at the higher energies.

At least part of the difference between the TDCC and the other two close-coupling calculations may be caused by a lack of correlation in the description of the target in the time-dependent calculations. The need for a $2s$ pseudo-orbital to avoid unphysical filling of the $1s$ orbital does not allow us to include any two-electron correlations $(2s^2 + 2p^2 + \cdots)$ in our target description. On the other hand, the CCC and RMPS calculations both include ground-state correlations. However, this does not explain the smaller difference between the RMPS and CCC calculations.

In Fig. 1(b), we present ionization cross sections for electron scattering from the first excited $1s^2 2s 2p$ configuration of beryllium. Again we present TDCC calculations as described and both sets of distorted-wave calculations as before. We also present RMPS calculations for ionization from the $2s 2p$ ^3P metastable term. All calculations include ionization contributions from both the $2s$ and $2p$ subshells. For this configuration, the TDCC and RMPS calculations are in quite good agreement in the threshold region. The two sets of calculations may start to differ at higher energies. Unfortunately, we cannot test this since the RMPS calculations cannot be extended to the higher energies considered here due to computational restrictions on the number of pseudostates that can be included as well as limits on the size of the basis set used to represent the $(N+1)$-electron continuum.

It is interesting that the configuration-average TDCC calculations are in such good agreement with the RMPS calculations made from the ^3P term of the $2s 2p$ configuration. This indicates that the $2s$ and $2p$ orbitals used in the TDCC calculations are very similar to the $2s$ and $2p$ orbitals which make up the ^3P metastable term. However, it should be mentioned that the time-dependent calculations presented here for neutral Be should be considered as a first step towards a complete description of ionization using the TDCC method. A much more extensive three-electron calculation would be necessary to provide a full treatment of ground-state correlation and term dependence in the $2s 2p$ excited states.

The nonperturbative calculations shown in Fig. 1(b) are almost a factor of 2 lower than the distorted-wave calculations in the region of the peak of the cross section. The sharp rise in the DWIS(N) cross section at around 10 eV is due to the very sharp onset of ionization from the $2s$ subshell, which has a much more gradual onset when calculated by the other methods. Again, at the highest energies considered (over 15 times the ionization threshold), the distorted-wave calculations are in good agreement with the TDCC calculations, due to the increasing contribution from the higher partial waves at these energies.

Unfortunately, there are no experimental measurements with which to compare for ionization from any configuration of neutral beryllium. A series of experimental measurements, although difficult for this toxic element, would prove very beneficial. However, by comparing perturbative calculations
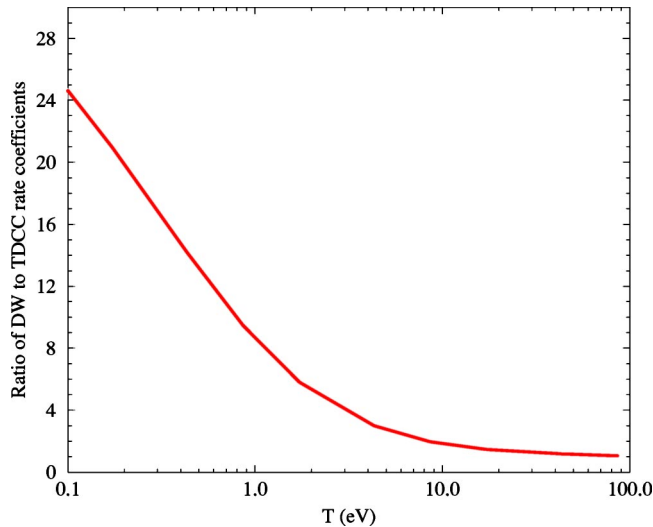
FIG. 2. Ratio of the direct ionization rate coefficients calculated using the DWIS(N) method to the rate coefficients calculated using the TDCC method for neutral Be($2s^2$). The ratio is plotted as a function of the electron temperature in eV.

with more sophisticated nonperturbative calculations, and by exploring any differences between these, an accurate database of ionization cross sections and rates may be constructed.

The cross sections presented in Fig. 1 are generally converted into ionization rate coefficients when used in a collisional-radiative modeling calculation. This involves integrating the cross section with a Maxwellian temperature distribution. The collisional ionization equilibrium region, which is the region where ionization and recombination are approximately equal, is typically around an order of magnitude below the ionization threshold of the ground configuration. Hence the low-energy region of the cross section is very important in modeling any plasma. This is especially true in astrophysics, where many cosmic plasmas are in collisional ionization equilibrium [33]. Ionization can occur below the ionization threshold of the ground state due to the width of the electron Maxwellian distribution. In Fig. 2, we present the ratio of the rate coefficient calculated using the DWIS(N) cross sections to the rate coefficient calculated using the TDCC cross sections for ionization out of the $2s^2$ ground state. The ratio of over 10 below about 0.8 eV highlights the large differences at low temperatures between cross sections calculated using the two methods. These direct ionization rate coefficients, which, together with excitation and recombination rate coefficients and collisional data from excited levels, go into the collisional radiative model and emphasize the need for nonperturbative calculations for neutral atoms.

B. Electron-impact ionization of Be$^+(1s^2 2s)$ and $(1s^2 2p)$

In Fig. 3, we present electron-impact ionization cross sections for lithiumlike Be$^+$ from (a) the ground $1s^2 2s$ and (b) the first excited $1s^2 2p$ states. We note that a study of electron-impact ionization of Be$^+$ from the ground state using both the time-dependent close-coupling and R-matrix
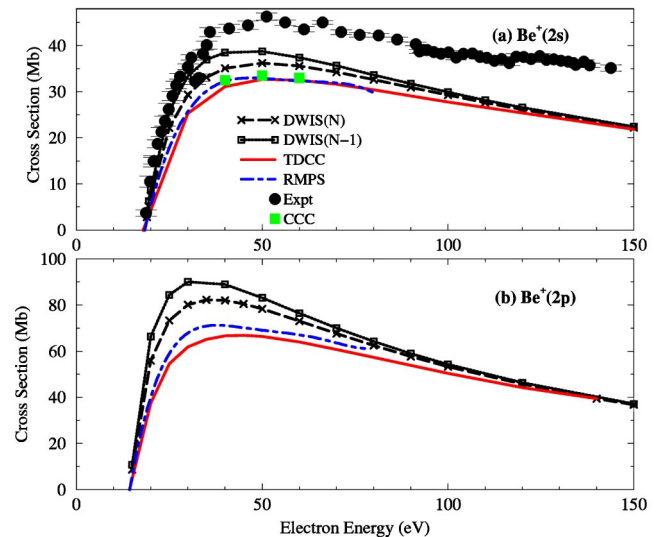

FIG. 3. Electron-impact ionization cross sections for Be$^+$ from (a) the ground $1s^2 2s$ configuration and (b) the first excited $1s^2 2p$ configuration. The solid lines are the time-dependent close-coupling calculations. The long-dashed lines (with crosses) are the DWIS(N) calculations and the dotted lines (with squares) are the DWIS($N-1$) calculations. The dot-dashed lines are R-matrix with pseudostates calculations, the solid squares are CCC calculations from [34], and the experimental measurements are from Ref. [6] (1.0 Mb$=1.0\times 10^{-18}$ cm^2).

with pseudostates methods has already been made by Pindzola *et al.* [11]. However, in the interests of completeness, we confirm and extend these calculations for Be$^+$. Also, we see trends in our work on this ion that are similar to our previous calculations on the ground and first excited states of lithium [13].

Our TDCC calculations were made again using a uniform mesh of $\Delta r = 0.2$ with 512 mesh points. The Fourier-transform technique was also employed to extract ionization cross sections over a wide range of incident-electron energies. The pseudopotential employed to construct the $2s$ orbital, in a manner similar to the previous set of calculations, was tuned to the experimental value of 18.21 eV [32] for ionization from Be$^+(2s)$. The ionization threshold for ionization from the $2p$ state of Be$^+$ was tuned to be 14.25 eV, also in good agreement with experiment.

For the new RMPS calculations for this ion, three spectroscopic orbitals and 57 pseudo-orbitals up to $n=14$ were included in the target description. A total of 42 basis orbitals were used to represent the $(N+1)$-electron continuum for each value of the angular momentum and the size of the R-matrix box was 42.0 a.u. In this ion, we carried out several RMPS calculations in which we varied the Laguerre pseudoorbitals in order to study the sensitivity of the resulting ionization cross section to the energies of the pseudo-states. We found variations in the cross sections of the order of 5% between these calculations. For the RMPS results presented here, the pseudostates were adjusted until they were spaced equally about the ionization limit, since this tends to reduce the amount of bound character included in the positive-energy pseudostates. However, this sensitivity study is useful in providing some estimate of the uncertainty in the RMPS

ionization cross section arising from the choice of the pseudostate basis.

In Fig. 3(a), we present the new TDCC calculations for ionization from the 2s ground state for incident-electron energies from 30 to 150 eV. The TDCC calculations are in good agreement with the RMPS calculations performed from threshold to 79 eV, with the largest discrepancy at 40 eV where the TDCC results are about 4% below those from the RMPS calculation. We confirm that the present TDCC results are also in excellent agreement with the TDCC results presented in Ref. [11], although the current calculations have been made with larger box sizes and increased angular momenta in the close-coupling expansions. This also holds true for the agreement between the present and earlier RMPS results, although the current RMPS calculation was carried out with a larger pseudostate basis. We further note from this figure that our calculations are also in good agreement with earlier CCC calculations [34].

DWIS(N) and DWIS($N-1$) calculations are also presented, and found to be higher than the nonperturbative calculations near the peak of the cross section, although there is good agreement between the perturbative and nonperturbative calculations at the highest energies considered. For the case of Be$^+$(2s), there are also experimental measurements available, the only measurements for any of the Be species considered in this study. The measurements of Falk and Dunn [6] are shown as black circles in Fig. 3(a); these measurements are up to 30% higher than all the theoretical calculations over the entire energy range considered. As discussed in Ref. [11], the excellent agreement between different close-coupling calculations is a good evidence for the need of the experimental measurements for Be$^+$ to be reexamined.

In Fig. 3(b), we present electron-impact ionization cross sections for Be$^+$ from its first excited state $1s^2 2p$. Again we present TDCC calculations over a wide range of impact energies, from 20 to 140 eV, and the RMPS results over a more restricted range from threshold to 75 eV. The same mesh was used in this TDCC calculation as in the calculation from the 2s ground state, although again for this case, three times as many angular-momenta channels are coupled due to the $l_t = 1$ nature of the target. The TDCC calculations are in excellent agreement with RMPS calculations at 20 eV, but are slightly below the RMPS results (about 9%) at the peak in the TDCC cross section. Both are lower than both sets of distorted-wave calculations, DWIS(N) and DWIS($N-1$), around the peak of the cross section, although there is good agreement at the highest energies considered. We note that the magnitude of the ionization cross section from Be$^+$ (2p) is around twice as large as that from the ground (2s) state, as noted previously for neutral lithium [13].

In Fig. 4, we also present the ratio of the rate coefficient calculated using fitted DWIS(N) cross sections to the rate coefficient calculated using fitted TDCC cross sections, for ionization out of the 2s ground state of Be$^+$. The ratio is smaller than that obtained for neutral Be (Fig. 2), but is still significantly higher than 1.0 in the low-temperature region. This again reflects the large differences at low temperatures between cross sections calculated using the two methods.
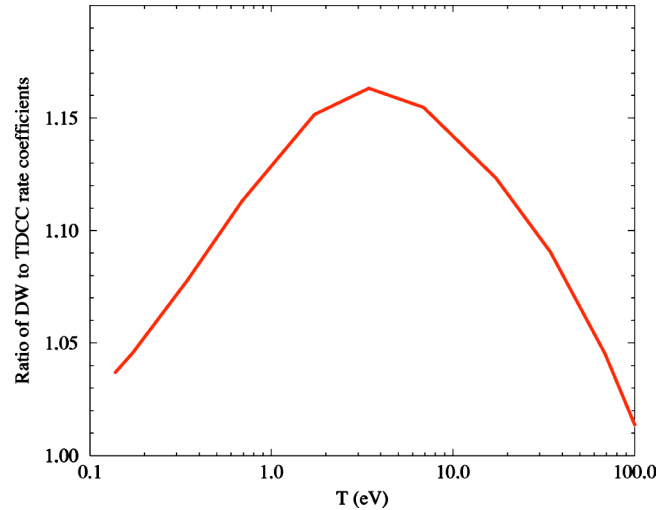

FIG. 4. Ratio of the direct ionization rate coefficients calculated using the DWIS(N) method to the rate coefficients calculated using the TDCC method for ground state Be$^+$(2s). The ratio is plotted as a function of the electron temperature in eV.

C. Electron-impact ionization of Be^{2+}($1s^2$) and ($1s2s$)

In Fig. 5, we present electron-impact ionization cross sections from heliumlike Be^{2+} from (a) the ground $1s^2$ and (b) the first excited $1s2s$ configuration. Again we show results from two sets of distorted-wave calculations, and nonperturbative TDCC and RMPS calculations. For this twice-ionized system, the distorted-wave calculations can be expected to become more accurate as the nuclear term of the potential begins to dominate the electronic term. For this case, the TDCC calculations were still made with 512 mesh points,
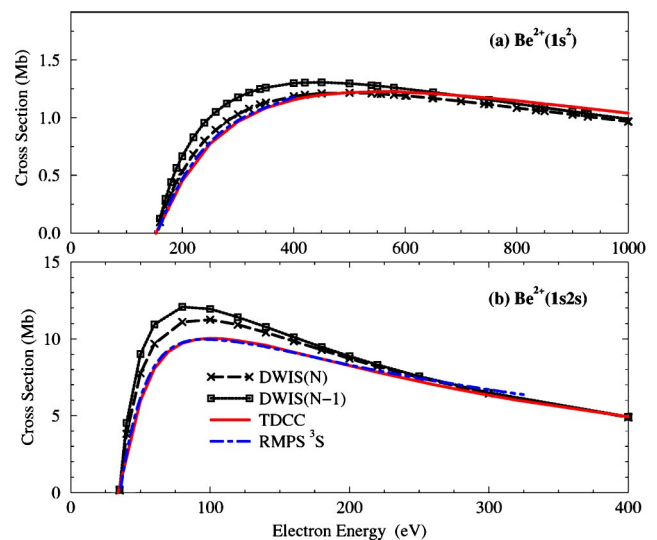

FIG. 5. Electron-impact ionization cross sections for Be^{2+} from (a) the ground $1s^2$ configuration and (b) the first excited $1s2s$ configuration. The solid lines are the time-dependent close-coupling calculations. The long-dashed lines (with crosses) are the DWIS(N) calculations and the dotted lines (with squares) are the DWIS($N-1$) calculations. The dot-dashed lines are the RMPS calculations (1.0 Mb = 1.0×10^{-18} cm^2).

although now with a uniform mesh spacing of $\Delta r = 0.1$, which was necessary to obtain accurate orbital energies. This reflects the fact that the two $1s$ electrons are tightly bound to the $Z=4$ nucleus in this case, necessitating a smaller mesh spacing in this region. The $1s$ hydrogenic orbital of Be^{3+} was first calculated and then a complete set of radial orbitals for heliumlike Be^{2+} was obtained by diagonalization of the single-particle Hamiltonian given by Eq. (4). A parameter in the exchange potential was adjusted to ensure that the single-particle energies are in good agreement with experimental measurements. For the ground state of Be^{2+}, the ionization threshold was 153.85 eV, in good agreement with the experimental measurement. For the $1s2s$ first excited configuration, the ionization threshold was 34.03 eV, again in fair agreement with the configuration-average experimental value. In the RMPS calculations, 60 spectroscopic and pseudo-orbitals were included in the target description, resulting in 119 terms; in addition, 52 basis orbitals were used to represent the $(N+1)$-electron continuum for each value of the angular momentum, and the size of the R matrix box was 27.4 a.u.

In Fig. 5(a), we show the ionization cross section from the ground state. It is evident that the TDCC and RMPS calculations are in excellent agreement over all energies considered. Also, the distorted-wave results are in fairly good agreement with the results from the nonperturbative calculations, especially for the DWIS(N) calculation. As expected, the distorted-wave calculations are becoming more accurate as the charge state increases.

For ionization from the $1s2s$ excited configuration shown in Fig. 5(b), the configuration-average TDCC and RMPS calculations from the metastable ^3S state are again in excellent agreement over the range of all energies considered. In this case, the DWIS(N) calculations are higher by around 20% in the region of the peak of the cross section, although again at higher energies they are in very good agreement with both nonperturbative calculations.

D. Electron-impact ionization of $Be^{3+}(1s)$ and $(2s)$

Finally, in Fig. 6 we present ionization of hydrogenlike Be^{3+}, again from (a) the ground $(1s)$ and (b) the first excited $(2s)$ states. In this case, we show an RMPS calculation and the two sets of distorted-wave calculations. In the RMPS calculation, 60 spectroscopic and pseudo-orbitals were included, 48 basis orbitals were used to represent the $(N+1)$-electron continuum for each value of the angular momentum, and the size of the R-matrix box was 20.2 a.u. We did not calculate cross sections using the TDCC method in this case, as it can be expected that fairly accurate cross sections can be produced using the distorted-wave methods for this three-times-ionized species where the nuclear potential term will completely dominate the electron interaction term. This is supported by the fact that both sets of distorted-wave cross sections are in good agreement with the RMPS cross section, although the differences are somewhat larger for ionization from the 2s excited state. Furthermore, the similarity between the DWIS(N) and DWIS($N-1$) results demonstrates that the choice of potentials for the evaluation
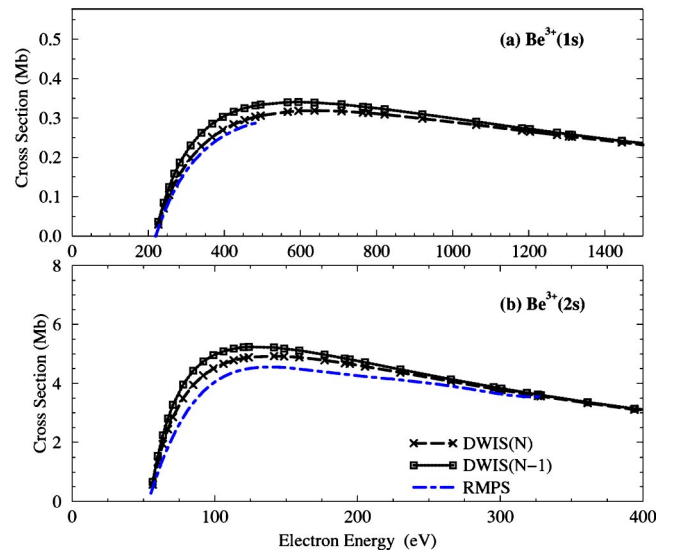

FIG. 6. Electron-impact ionization cross sections for Be^{3+} from (a) the ground $1s$ configuration and (b) the first excited $2s$ configuration. The long-dashed lines (with crosses) are the DWIS(N) calculations and the dotted lines (with squares) are the DWIS($N-1$) calculations. The dot-dashed lines are the RMPS calculations $(1.0 \text{ Mb} = 1.0 \times 10^{-18} \text{ cm}^2)$.

of the incident and scattered electrons makes a smaller difference to the ionization cross section in this case. Again, for this case, there are no experimental measurements with which to compare. We note that the magnitude of the cross sections in this case are appreciably smaller than in the previous ion stages, simply demonstrating the strength by which the electron is bound to the nucleus.

IV. SUMMARY

In this paper, we have presented a comprehensive set of theoretical calculations for the electron-impact ionization of beryllium and its ions, from both the ground and first excited configuration of all systems. For neutral Be, the time-dependent close-coupling and R-matrix with pseudostates calculations were compared with previous convergent close-coupling calculations. For Be^+, the TDCC and RMPS were compared with an older set of experimental measurements. For Be^{2+} the TDCC and RMPS calculations were in excellent agreement. For Be^{3+}, only RMPS calculations were presented, and for all cases these nonperturbative calculations were compared with two sets of distorted-wave calculations. These ionization data have now been inserted into the atomic data and analysis structure (ADAS) database [35] and will be made available to other atomic databases as required.

Although this work represents a significant step forward in the ionization data for Be and its ions, more work still remains to calculate accurate electron-ion scattering data for these systems. Nonperturbative calculations are necessary for ionization from more highly excited states, especially in neutral Be and in Be^+. Also, RMPS calculations of electron-impact excitation cross sections for Be^+ and Be^{2+}, as well as neutral Be, are now well underway. The calculations for the ions of beryllium are being done separately from these

ionization calculations, since a larger number of spectroscopic orbitals have to be included in the target description. These results will be reported later and will be compared to TDCC results for excitation above the resonance region, which are produced automatically in the TDCC calculations presented here. The collisional radiative model also requires accurate recombination data. Calculations of dielectronic recombination of Be^+, Be^{2+}, and Be^{3+} have already been made [36] as part of a larger project to calculate dielectronic recombination for many isoelectronic sequences of astrophysical and fusion interest. This work is nearing completion of a series of calculations on dielectronic recombination of elements in the first row of the periodic table and further calculations are planned.

Once all the electron-ion scattering calculations are completed, the full impact of these sets of nonperturbative results on the collision-radiative model for beryllium can be assessed. These new data, which should represent a significant improvement on the existing database (which was largely derived from semiempirical fits), represent a step forward in efforts to accurately model fusion plasma devices. Still, much work remains to be done on other light elements of fusion interest. Boron and carbon have been used as plasma-facing materials for the reactors walls; however, our knowledge of ionization and excitation rate coefficients for these systems and their ions is far from complete. More extensive nonperturbative calculations of ionization and excitation of light elements such as oxygen and nitrogen, as well as their ions (which may act as impurities within the plasma) are needed, although some recent progress has recently ben made for ionization calculations of oxygen ions [37]. Also, collisional data are necessary for the noble gases, especially neon and argon, which have been used as disruption mitigators in some fusion plasma devices.

Ionization and excitation calculations for these more complex systems require not only larger nonperturbative calculations but some theoretical development. For example, developments in the TDCC method are required in order to accurately describe electron-impact ionization (and excitation) from open shell systems containing several terms in the configuration. Although the current configuration-average approach can be modified by multiplication of an appropriate branching ratio to obtain the ionization from a particular term, the accurate description of a continuum electron with the remaining core electrons in an open shell remains an outstanding problem. Work on this is in progress.

ACKNOWLEDGMENTS

---

[1] W. Mandl, R. Wolf, M. von Hellermann, and H.P. Summers, Plasma Phys. Controlled Fusion **35**, 1371 (1993).

[2] J. Colgan, M.S. Pindzola, S.D. Loch, F. Robicheaux, and D.C. Griffin, in *Atomic Processes in Plasmas*, edited by D.R. Schultz, F.W. Meyer, and F. Ownby, AIP Conf. Proc. No. 635 (AIP, Melville, NY, 2002), p. 145.

[3] S.D. Loch, J. Colgan, M.S. Pindzola, C.P. Ballance, D.C. Griffin, D.M. Mitnik, M.G. O'Mullane, H.P. Summers, and A.D. Whiteford, Phys. Scr., (to be published).

[4] H. Bolt, V. Barabash, G. Federici, J. Linke, A. Loarte, J. Roth, and K. Sato, J. Nucl. Mater. **307**, 43 (2002).

[5] S.M. Younger, Phys. Rev. A **24**, 1278 (1981).

[6] R.A. Falk and G.H. Dunn, Phys. Rev. A **27**, 754 (1983).

[7] D.V. Fursa and I. Bray, J. Phys. B **30**, L273 (1997).

[8] D.V. Fursa and I. Bray, J. Phys. B **30**, 5895 (1997).

[9] K. Bartschat, P.G. Burke, and M.P. Scott, J. Phys. B **29**, L769 (1996).

[10] K. Bartschat, P.G. Burke, and M.P. Scott, J. Phys. B **30**, 5915 (1997).

[11] M.S. Pindzola, F. Robicheaux, N.R. Badnell, and T.W. Gorczyca, Phys. Rev. A **56**, 1994 (1997).

[12] K. Bartschat and I. Bray, J. Phys. B **30**, L109 (1997).

[13] J. Colgan, M.S. Pindzola, D.C. Griffin, and I. Bray, Phys. Rev. Lett. **87**, 213201 (2001).

[14] J. Colgan and M.S. Pindzola, Phys. Rev. A **66**, 062707 (2002).

[15] M.S. Pindzola, D.C. Griffin, and C. Bottcher, in *Atomic Processes in Electron-Ion and Ion-Ion Collisions*, Vol. 145 of *NATO Advanced Studies Institute, Series B: Physics*, edited by F. Brouillard (Plenum, New York, 1986), p. 75.

[16] M.S. Pindzola and D.R. Schultz, Phys. Rev. A **53**, 1525 (1996).

[17] M.S. Pindzola and F. Robicheaux, Phys. Rev. A **54**, 2142 (1996).

[18] M.S. Pindzola, F. Robicheaux, J. Colgan, D.M. Mitnik, D.C. Griffin, and D.R. Schultz, in *Proceedings of the 22nd International Conference on Photonic, Electroic, and Atomic Collisions*, edited by J. Burgdörfer, J.S. Cohen, S. Datz, and C.R. Vane (Rinton Press, Princeton, NJ, 2002), p. 483.

[19] K.A. Berrington, W.B. Eissner, and P.H. Norrington, Comput. Phys. Commun. **92**, 290 (1995).

[20] T.W. Gorczyca and N.R. Badnell, J. Phys. B **30**, 3897 (1997).

[21] D.M. Mitnik, M.S. Pindzola, D.C. Griffin, and N.R. Badnell, J. Phys. B **32**, L479 (1999).

[22] D.M. Mitnik, C.P. Ballance, D.C. Griffin, and N.R. Badnell, J. Phys. B **36**, 717 (2003).

[23] N.R. Badnell, D.C. Griffin, and D.M. Mitnik, J. Phys. B **36**, 1337 (2003).

[24] R.D. Cowan, *The Theory of Atomic Structure and Spectra* (University of California Press, Berkeley, 1981).

[25] M.E. Riley and D.G. Truhlar, J. Chem. Phys. **63**, 2182 (1975).

[26] J. Botero and J.H. Macek, J. Phys. B **24**, L405 (1991).

[27] M.S. Pindzola, J. Colgan, F. Robicheaux, and D.C. Griffin, Phys. Rev. A **62**, 042705 (2000).

[28] M.S. Pindzola, F. Robicheaux, N.R. Badnell, and T.W. Gorczyca, Phys. Rev. A **56**, 1994 (1997).

[29] J. Colgan, M.S. Pindzola, and F. Robicheaux, Phys. Rev. A **66**, 012718 (2002).

[30] K. Bartschat, Comput. Phys. Commun. **114**, 168 (1998).

[31] N.R. Badnell, J. Phys. B **19**, 3827 (1986).

[32] C.E. Moore, *Atomic Energy Levels I*, Natl. Bur. Stand. (U.S.) Circ. No. 35 (U.S. PO, Washington, D.C., 1971), Vol. I.

[33] S.M. Kahn, E. Behar, A. Kinkhabwala, and D.W. Savin, Philos. Trans. R. Soc. London, Ser. A **360**, 1923 (2002).

[34] I. Bray, J. Phys. B **28**, L247 (1995).

[35] H.P. Summers, ADAS Manual V2. 5, http://adas.phys.strath.ac.uk/ (2002).

[36] N.R. Badnell, M. O'Mullane, H.P. Summers, Z. Altun, M.A. Bautista, J. Colgan, T.W. Gorczyca, D.M. Mitnik, M.S. Pindzola, and O. Zatsarinny, Astron. Astrophys. **406**, 1151 (2003).

[37] S.D. Loch, J. Colgan, M.S. Pindzola, M. Westermann, F. Scheuermann, K. Aichele, D. Hathiramani, and E. Salzborn, Phys. Rev. A **67**, 042714 (2003).